Journal of Applied Spectroscopy, Vol. 74, No. 6, 2007

TWO-PERIOD MODEL FOR CALCULATION OF LEVEL POPULATIONS IN SUBBANDS OF MULTI-PERIOD QUANTUM-CASCADE SUPERLATTICE STRUCTURES

D. V. Ushakov* **and I. S. Manak**

UDC 535.374:621.375.8

For two periods of quantum-cascade laser structures, we propose a system of closed balance equations that make it possible to calculate the occupancy of the energy levels, the quasi-Fermi levels, and also the injection current density taking into account different charge carrier scattering mechanisms.

Key words: *quantum-cascade laser, energy level population, charge carrier scattering, system of closed balance equations.*

Introduction. Development of lasers based on quantum-cascade superlattice structures is a promising direction in design of compact and reliable radiation sources in the mid-IR [1–5] and far IR [6, 7] ranges. The design concept for a quantum-cascade laser (QCL) was discussed in [8], but the first practical realization is described in [1]. Modern QCLs are grown using the molecular beam epitaxy method and are complicated structures with several tens of repeating cascades, consisting of a system of potential wells and barriers. The populations of the energy subbands are calculated based on solution of balance equations in the approximation of two or three [4, 9, 10] minisubbands or in the multi-subband self-consistent approximation [11, 12]. In this case, calculations of the scattering rates use the Monte Carlo method [13] and also the Green's function method [14], incurring significant computation costs. In this paper, we propose a system of closed balance equations to determine the energy level populations for only two periods of the QCL, which allows us to take into account all possible transitions between levels and the coupling between cascades, and also to reduce computation costs and shorten calculation time.

Calculation. The algorithm for calculating the optoelectronic properties of QCLs includes the following steps: solution of the Schrodinger equation and determination of the energy levels and wavefunctions; calculation of the dipole transition matrix elements; calculation of the rates of scattering off optical phonons and electron-electron scattering; determination of the surface concentrations of charge carriers and quasi-Fermi levels for the corresponding energy subbands from a system of closed balance equations; calculation of threshold currents and spectral characteristics.

Figure 1a shows the results of a numerical calculation of the conduction band diagram $E_c(z)$ and the modulus squared of the electron wavefunctions for two periods of the QCL. The parameters of the band structure and the thicknesses of the layers are taken from [2]. The values of the modulus squared of the wavefunctions corresponding to the N-th period are numbered. For convenience in calculating the level populations of the subbands, the QCL period should be understood to mean the repetition period of the system of wavefunctions, which may be greater than the thickness of one cascade (the repetition period of the potential wells and barriers), since the wavefunctions extend over several cascades. As we see, two periods of the squares of the wavefunctions corresponds to about three cascades in the structure.

The optical transitions occur between energy levels in each period and between periods. For the quantum-cascade structure calculated in Fig. 1a, the fundamental frequency of the QCL emission (~134 meV) corresponds to an optical transition of an electron from the first level of the $(N - 1)$-th period to the 11th level of the N-th period, i.e., 1, $(N - 1)$ — 11, N. In this case, as we see from Fig. 1b, the dipole matrix element is 5.7 nm.

*To whom correspondence should be addressed.

Belorussian State University, 4 prosp. Nezavisimosti, Minsk 220030. E-mail: UshakovDV@bsu.by. Translated from Zhurnal Prikladnoi Spektroskopii, Vol. 74, No. 6, pp. 801–804, November–December, 2007. Original article submitted May 7, 2007.

 0021-9037/07/7406-0892 ©2007 Springer Science+Business Media, Inc.

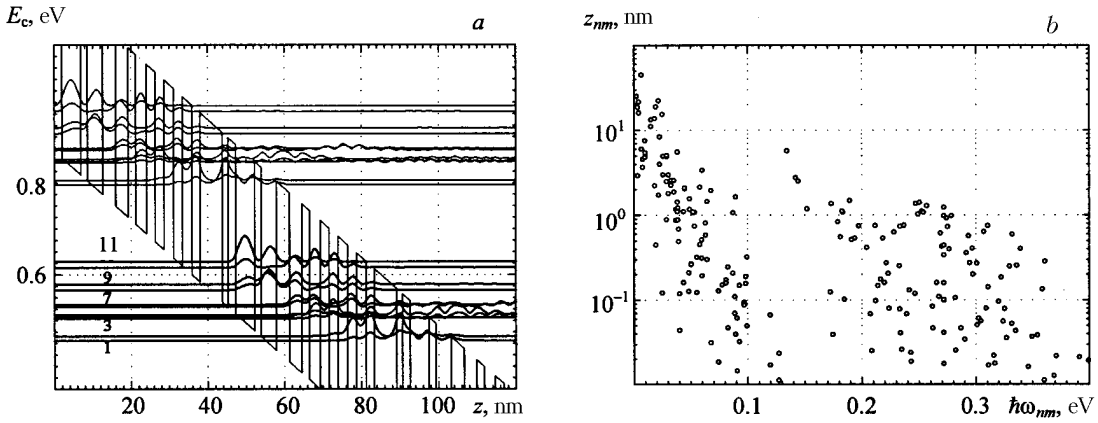

Fig. 1 Distribution of $E_c(z)$ in the conduction band and the modulus squared of the electron wavefunctions (a), and also the transition dipole matrix elements z_{nm} with energies $\hbar\omega_{nm}$ (b) for two cascades of the superlattice structure of $Al_{33}Ga_{0.67}As$–GaAs in an electric field of strength $E = 6\cdot10^6$ V·m^{-1}. The thicknesses (in nm) of the layers of the structure in sequence from left to right are: /2.0/**4.9**/1.7/4.0/3.4/**3.2**/2.0/**2.8**/2.3/**2.3**/2.5/**2.3**/2.5/**2.1**/5.8/**1.5**/, where the GaAs quantum wells are identified in boldface.

In determining the occupancy of the subbands, we assume that a quasi-Fermi level F_n and a surface electron concentration n_{sn} corresponds to each energy level E_n, and these parameters are determined from the following system of balance equations:

$$\frac{dn_{i_N}}{dt} = \sum_{j_N \neq i_N} \left(R_{j_N i_N} - R_{i_N j_N} \right) + \sum_{j_{N-1}} \left(R_{j_{N-1} i_N} - R_{i_N j_{N-1}} \right) + \sum_{j_{N+1}} \left(R_{j_{N+1} i_N} - R_{i_N j_{N+1}} \right), \quad i_N = 1 \ldots n_{\max} - 1 ,$$

$$\sum_{i_N=1}^{n_{\max}} n_{si_N} = n_{st} . \tag{1}$$

Here the first sum corresponds to the difference between the arrival rate $R_{j_N i_N}$ at level i from all j and the departure rate $R_{i_N j_N}$ from i to all j levels in the N-th period. The second sum determines the difference between the rates of electron arrival and departure at the i level of the N-th period from all the j levels of the $(N - 1)$-th period; the third sum determines the difference between the rates of electron arrival and departure at the i level of the N-th period from all the j levels of the $(N + 1)$-th period. The latter equation includes the sum of the surface electron concentrations n_{si_N} at all levels of the N-th period, equal to n_{st}. Note that the value of n_{st} is induced by impurities and is determined by the doping of the emitters. Since the energy levels and wavefunctions in all the QCL periods are identical, their occupancies can also be considered identical. In this case, transitions of electrons from the N-th to the $(N + 1)$-th period are equivalent to transitions of electrons from the $(N - 1)$-th to the N-th period, which allows us to calculate the wavefunctions for only two QCL periods. The system of equations (1) was solved for the steady-state case, when $\frac{dn_{i_N}}{dt} = 0$.

The quasi-Fermi levels and the surface concentrations of the electrons are interconnected by the relation

$$n_{sn} = \frac{m_c kT}{\pi\hbar^2} \ln\left(1 + \exp\left[\frac{F_n - E_n}{kT}\right]\right). \tag{2}$$

The total injection current density J is defined as

$$J = \sum_{i_N} J_{i_N} = e \sum_{i_N} \sum_{j_{N-1}} \left(R_{j_{N-1} i_N} - R_{i_N R_{j_{N-1}}} \right), \tag{3}$$

where $J_{i_N} = \eta_{i_N} J$ is the injection current density for the i-th level of the N-th period, η_{i_N} is the corresponding injection coefficient, determining the fraction of injected electrons. The integrated transition rates R_{ij} are found by summing the transitions, taking into account all possible scattering mechanisms. In a QCL, the major scattering mechanism is scattering off polar optical phonons at the rate

$$S_{if}^{\text{oph}\pm}(E_i) = \frac{e^2 \omega_q}{8\pi\varepsilon_0} \left(\frac{1}{\varepsilon_\infty} - \frac{1}{\varepsilon} \right) \left(N_q + \frac{1}{2} \pm \frac{1}{2} \right) \int_{-\infty}^{+\infty} dq_z \left| \int_0^d e^{-iq_z z} \psi_i(z) \psi_f^*(z)\, dz \right|^2 \tag{4}$$

$$\times \frac{1}{\left(\left(E_i - E_{in} + \left(E_i \mp \hbar\omega_q - E_{fm} \right) + E_{q_z} \right)^2 - 4 (E_i - E_{in}) \left(E_i \mp \hbar\omega_q - E_{fm} \right) \right)^{\frac{1}{2}}},$$

where $E_{q_z} = \dfrac{\hbar^2 q_z^2}{2m_c}$; $\hbar\omega_q$ is the energy of the polar optical phonon; $N_q = \left(\exp\left[\dfrac{\hbar\omega_q}{kT} \right] - 1 \right)^{-1}$ is the phonon occupancy number; ε_∞ and ε are the optical and static dielectric constants. The integrated transition rate is defined as

$$R_{if}^{\text{oph}\pm} = \frac{n_c}{\pi\hbar^2} \int dE\, H(E - E_n)\, f(E - F_n) \left(1 - f\left(E \mp \hbar\omega_q - F_m \right) \right) S_{if}^{\text{oph}\pm}(E). \tag{5}$$

Here $H(E)$ is the Heaviside step function; $f(E) = \left(\exp\left[\dfrac{E}{kT} \right] + 1 \right)^{-1}$ is the Fermi–Dirac distribution function.

For QCLs operating in the far IR range, we need to also take into account electron-electron scattering with transition rate [15]

$$R_{ijfm}^{\text{ee}} = (2\pi)^2 \,\text{Ry}\, \hbar \frac{n_i n_j}{m_0 \varepsilon^2} \frac{\left| F_{ijfm}(g_0/2) \right|^2}{E_{\text{S}}}, \tag{6}$$

where the n_i are the surface concentrations of electrons at the i-th energy level; Ry ≈ 13.6 eV; $g_0^2 = 8 m_{\text{r}} E_{\text{S}} / \hbar^2$, $E_{\text{S}} = E_i + E_j - E_f - E_m$; m_{r} is the reduced effective mass. The form factor for overlap of the wavefunction envelopes $F_{ijfm}(q)$ is defined according to [13]:

$$F_{ijfm}(q) = \iint dz_1 dz_2 \psi_f^*(z_1) \psi_m^*(z_2) e^{-q|z_1 - z_2|} \psi_i(z_1) \psi_j(z_2). \tag{7}$$

Discussion of Results. Table 1 and Fig. 2 show the results of numerical solution of the system of closed balance equations for different threshold surface concentrations of electrons in one period n_{st} for fixed electric field strength $E = 6 \cdot 10^6$ V·m^{-1}. As shown by the calculations, levels 1 and 2 have higher occupancies than the rest, with surface concentrations of electrons ~10^{10}–10^{11} cm^{-2} depending on the excitation level, which is consistent with experimental data [2]. The injection currents and accordingly the injection coefficients are maximum for levels 11 and 8. Thus for level 11, as the total surface concentrations of electrons increases, n_{st} = $5 \cdot 10^{10}$, $1.5 \cdot 10^{11}$, and $2.5 \cdot 10^{11}$ cm^{-2}, the injection current densities also increase and are J_{11} = 451, 1359, and 2280 A·cm^{-2} respectively. We should point out that the injection coefficients η_i practically do not vary as the QCL pumping increases. This can be used to simplify the numerical calculations for the system of balance equations (1).

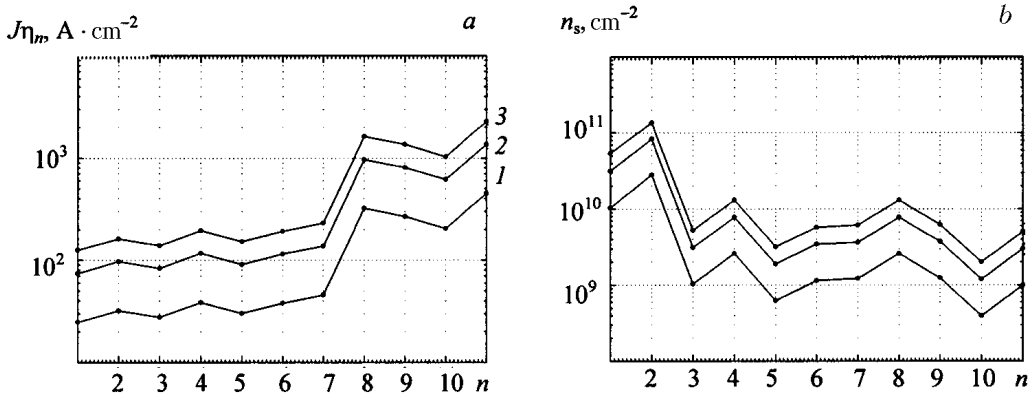

Fig. 2 Distribution of current densities $J\eta_n$ (a) and surface electron concentrations ns over the energy levels n (b) for different total surface electron concentrations in one cascade $n_{st} = 5\cdot10^{10}$ (1), $1.5\cdot10^{11}$ (2), and $2.5\cdot10^{11}$ (3) cm^{-2}; T = 77 K.

TABLE 1 Parameters of a Quantum-Cascade Laser for Different Pump Levels

n	1	2	3	4	5	6	7	8	9	10	11
E_n, meV	485	493	523	525	530	545	548	573	583	612	622
$\eta_n(10^{-3})$	16.7	21.7	18.7	26.1	20.4	25.7	30.8	21.7	181.0	137.9	304.4
$n_{st} = 5\cdot10^{10}$ cm^{-2}; J =1.48 kA·cm^{-2}											
F_n, meV	465	479	487	496	490	509	513	544	549	570	587
$n_{st} = 1.5\cdot10^{11}$ cm^{-2}; J = 4.46 kA·cm^{-2}											
F_n, meV	472	488	494	503	498	517	521	552	556	578	594
$n_{st} = 2.5\cdot10^{11}$ cm^{-2}; J = 7.48 kA·cm^{-2}											
F_n, meV	476	492	498	507	501	520	524	555	560	581	598

Note. $E = 6\cdot10^6$ V·m^{-1}, T = 77 K.

Conclusion. We propose an efficient procedure for modeling optoelectronic properties of quantum-cascade superlattice structures. We have carried out a numerical solution of a system of closed balance equations for two QCL periods. We have calculated the occupancy and the quasi-Fermi levels for the corresponding energy subbands, and also have analyzed the nature of the change in the injection current densities.

We would like to thank A. A. Afonenko for discussion of the results.

This work was done with the support of the Belorussian Republic Foundation for Basic Research.

REFERENCES

1. J. Faist, F. Capasso, D. L. Sivco, C. Sirtori, A. L. Hutchinson, and A. Y. Cho, *Science*, **264**, 553–556 (1994).
2. C. Sirtori, P. Kruck, S. Barbieri, P. Collot, J. Nagle, M. Beck, J. Faist, and U. Oesterle, *Appl. Phys. Lett.*, **73**, No. 24, 3486–3488 (1998).
3. C. Sirtori, P. Kruck, S. Barbieri, H. Page, J. Nagle, M. Beck, J. Faist, and U. Oesterle, *Appl. Phys. Lett.*, **75**, No. 25, 3911–3913 (1999).
4. F. Capasso, A. Tredicucci, G. Gmachl, D. L. Sivco, A. L. Hutchinson, A. Y. Cho, and G. Scamarcio, *IEEE J. Select. Top. Quantum Electron.*, **5**, No. 3, 792–807 (1999).

5. R. Teissier, D. Barate, A. Vicet, C. Alibert, A. N. Baranov, X. Marcadet, C. Renard, M. Garcia, C. Sirtori, D. Revin, and J. Cockburn, *Appl. Phys. Lett.*, **85**, No. 2, 167–169 (2004).
6. L. Ajili, G. Scalari, N. Hoyler, M. Giovannini, and J. Faist, *Appl. Phys. Lett.*, **87**, 141107-1–141107-3 (2005).
7. G. Scalaria, N. Hoyler, M. Giovannini, and J. Faist, *Appl. Phys. Lett*., **86**, 181101-1–181101-3 (2005).
8. R. A. Kazarinov and R. A. Suris, *Fiz. Tekh. Poluprovodn*., **6**, No. 1, 148–162 (1972).
9. V. B. Gorfinkel, S. Luryi, and B. Gelmont, *IEEE J. Quantum Electron*., **32**, No. 11, 1995–2003 (1996).
10. D. V. Ushakov and A. A. Afonenko, in: S. A. Maskevich, V. F. Stel'makh, and A. K. Fedotov, *Low-Dimensional Systems* [in Russian], Izdat. Grodn. Gos. Univ., Grodno (2003), No. 3, p. 29–34.
11. J. Faist, D. Hofstetter, M. Beck, T. Aellen, M. Rochat, and S. Blaser, *IEEE J. Quantum Electron*., **38**, No. 6, 533–546 (2002).
12. D. Indjin, P. Harrison, R. W. Kelsall, and Z. Ikonic, *J. Appl. Phys*., **91**, No. 11, 9019–9026 (2002).
13. M. Dur, S. M. Goodnick, and P. Lugli, *Phys. Rev. B*, **54**, No. 24, 17794–17804 (1996).
14. S.-C. Lee and A. Wacker, *Phys. Rev. B*, **66**, No. 24, 245314-1–245314-18 (2002).
15. A. N. Drozd and A. A. Afonenko, *Zh. Prikl. Spektr*., **72**, No. 6, 782–787 (2005).